Draft version May 1, 2024
Typeset using LaTeX **modern** style in AASTeX631

Hiding Out at the Low End: Gaps and Peaks in the Black-Hole Mass Spectrum
Hide and Seek ...

Will M. Farr[1,2] and Vassiliki Kalogera[3,4]

[1] *Department of Physics and Astronomy, Stony Brook University, Stony Brook, NY 11794, USA*
[2] *Center for Computational Astrophysics, Flatiron Institute, 162 Fifth Avenue, New York, NY 10010, USA*
[3] *Department of Physics and Astronomy, Northwestern University, 2145 Sheridan RD, Evanston, IL 60208, USA*
[4] *Center for Interdisciplinary Exploration and Research in Astrophysics (CIERA), Northwestern University, 1800 Sherman Ave, Evanston, IL 60201, USA*

ABSTRACT

It is not known whether there is a continuum of masses of compact objects formed from stellar collapse from the heaviest neutron stars to the lightest black holes or whether there is a gap in the mass spectrum between these classes of objects. The presence or absence of a mass gap has implications for the supernova mechanism, as well as being a fundamental property of the compact object mass function. In X-ray binaries containing black holes a gap is observed, but it is not known whether this is representative of a true gap in the mass function or due to selection effects or systematic biases in mass estimation. A small number of black holes have been observed with luminous companions in non-interacting orbits, but as yet the sample is too small to assess the existence of a gap, and in any case selection effects in this sample are hard to quantify TODO: Check this!. Binary black hole mergers detected from gravitational waves in the GWTC-3 transient catalog furnish a large sample of several tens of low-mass black holes with a well-understood selection function. Here we analyze the 26 GWTC-3 merger events with at least one black hole ($3\,M_\odot < m_1$) and chirp masses below those of a $20\,M_\odot$–$20\,M_\odot$ merger ($M_c < 17.41\,M_\odot$) to uncover the structure of the low-mass black hole mass function in these systems. Using flexible parameterized models for the mass function, we find a sharp peak in the mass function at $m = 9.26^{+0.55}_{-0.66}\,M_\odot$, associated with merger rates $m_1 m_2 \mathrm{d}N/\mathrm{d}m_1\mathrm{d}m_2\mathrm{d}V\mathrm{d}t = 129^{+159}_{-64}\,\mathrm{Gpc}^{-3}\,\mathrm{yr}^{-1}$. The mass function falls by about an order of magnitude both below and above this peak. Toward the lowest masses, the mass function may or

will.farr@stonybrook.edu
wfarr@flatironinstitute.org
vicky@northwestern.edu

may not flatten; we find that the 1% black hole mass in our most flexible model is $m_{1\%} = 3.61^{+1.63}_{-0.48}\,M_\odot$. In other words, this sample of low-mass black holes does not require a mass gap but may permit one; observations in the currently-ongoing "O4" observation run should distinguish these possibilities. Toward higher masses, the mass function declines steeply, with power law slopes $\mathrm{d}N/\mathrm{d}m \sim m^\alpha$, $\alpha = -2.2^{+1.3}_{-2.9}$. The presence of a peak at $m \sim 9\,M_\odot$ is suggested by several models of stellar evolution.

1. INTRODUCTION

Definition of our mass functions:

$$m_1 m_2 \frac{\mathrm{d}N}{\mathrm{d}m_1 \mathrm{d}m_2 \mathrm{d}V \mathrm{d}t} = R f\left(m_1\right) f\left(m_2\right) g(m_1, m_2) r(z) \tag{1}$$

The "common" mass function f takes either a broken power law form,

$$f(m) = \begin{cases} \left(\frac{m}{m_b}\right)^{\alpha_1} & m < m_b \\ \left(\frac{m}{m_b}\right)^{\alpha_2} & m_b < m \end{cases}, \tag{2}$$

or a sum of a broken power law and a Gaussian,

$$f(m) = f_g \exp\left(-\frac{(m-\mu)^2}{2\sigma^2}\right) + (1 - f_g) \begin{cases} \left(\frac{m}{\mu}\right)^{\alpha_1} & m < \mu \\ \left(\frac{m}{\mu}\right)^{\alpha_2} & \mu < m \end{cases}. \tag{3}$$

The "pairing function" (Fishbach & Holz 2020) g is a power law in the total mass,

$$g(m_1, m_2) = \left(\frac{1 + \frac{m_2}{m_1}}{2}\right)^\beta. \tag{4}$$

The redshift evolution is forced to follow a Madau-Dickinson star formation rate (Madau & Dickinson 2014)

$$r(z) = \frac{(1+z)^{2.7}}{1 + \left(\frac{1+z}{1+1.9}\right)^{5.6}} \left(1 + \left(\frac{1}{1+1.9}\right)^{5.6}\right). \tag{5}$$

With these definitions, R is the merger rate per natural log mass squared, per comoving volume, per time at redshift $z = 0$, $m_1 = m_2 = \mu, m_b$. We use the convention $m_2 \leq m_1$. The parameter α_1 is the power law slope of the mass function much below the break mass m_b or mean mass μ, α_2 is the power law slope of the mass function much above m_b or μ. The parameter β is the power law slope of the mass ratio in the pairing function[1]. The parameter f_g is the fraction of the merger

[1] We also explored Gaussian pairing functions,

$$g\left(m_1, m_2\right) \propto \exp\left(-\left(m_2/m_1 - \mu_q\right)^2 / \left(2\sigma_q^2\right)\right); \tag{6}$$

but found no qualitative and few quantitative differences with the results reported here.

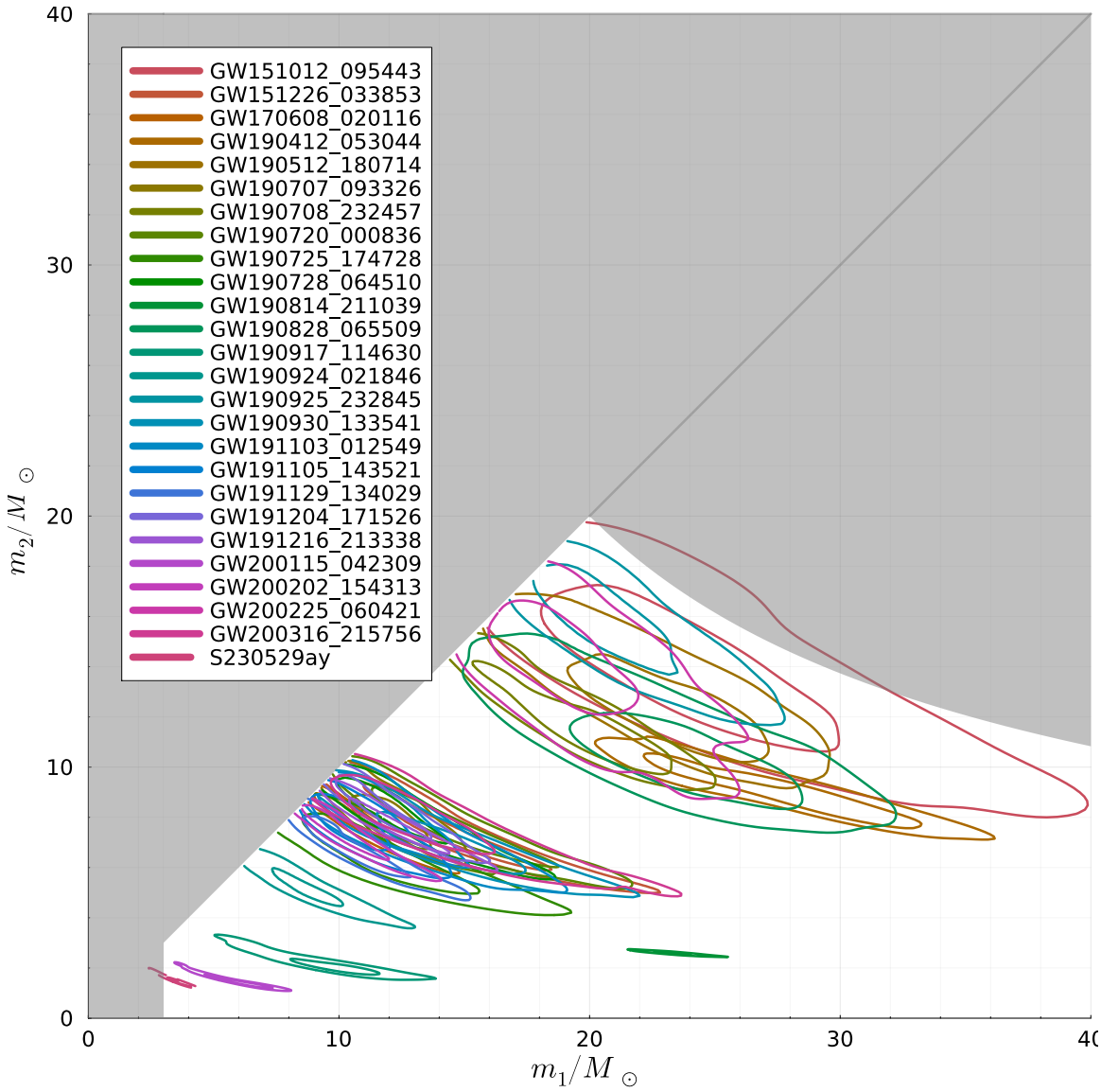

Figure 1. Contour plot of the likelihood functions for the primary and secondary black hole masses in the events considered in this analysis. The contours show credible regions containing 50% and 90% of the likelihood for each event. The dashed lines show our selection cuts, with $m_1 > 3\,M_\odot$ and $M_c < 17.41\,M_\odot$.

rate at $m_1 = m_2 = \mu$ that is in the Gaussian component of the mass function. When normalizing the "common" mass function f to be a probability distribution for $m_{\rm low} \leq m \leq m_{\rm high}$ we will write

$$p(m) \equiv \frac{f(m)}{\int_{m_{\rm low}}^{m_{\rm high}} {\rm d}m'\, f(m')}. \tag{7}$$

1 We thank Jeff Andrews for comments on an early version of this work.

Software: `zenodo-get` (Völgyes 2020)

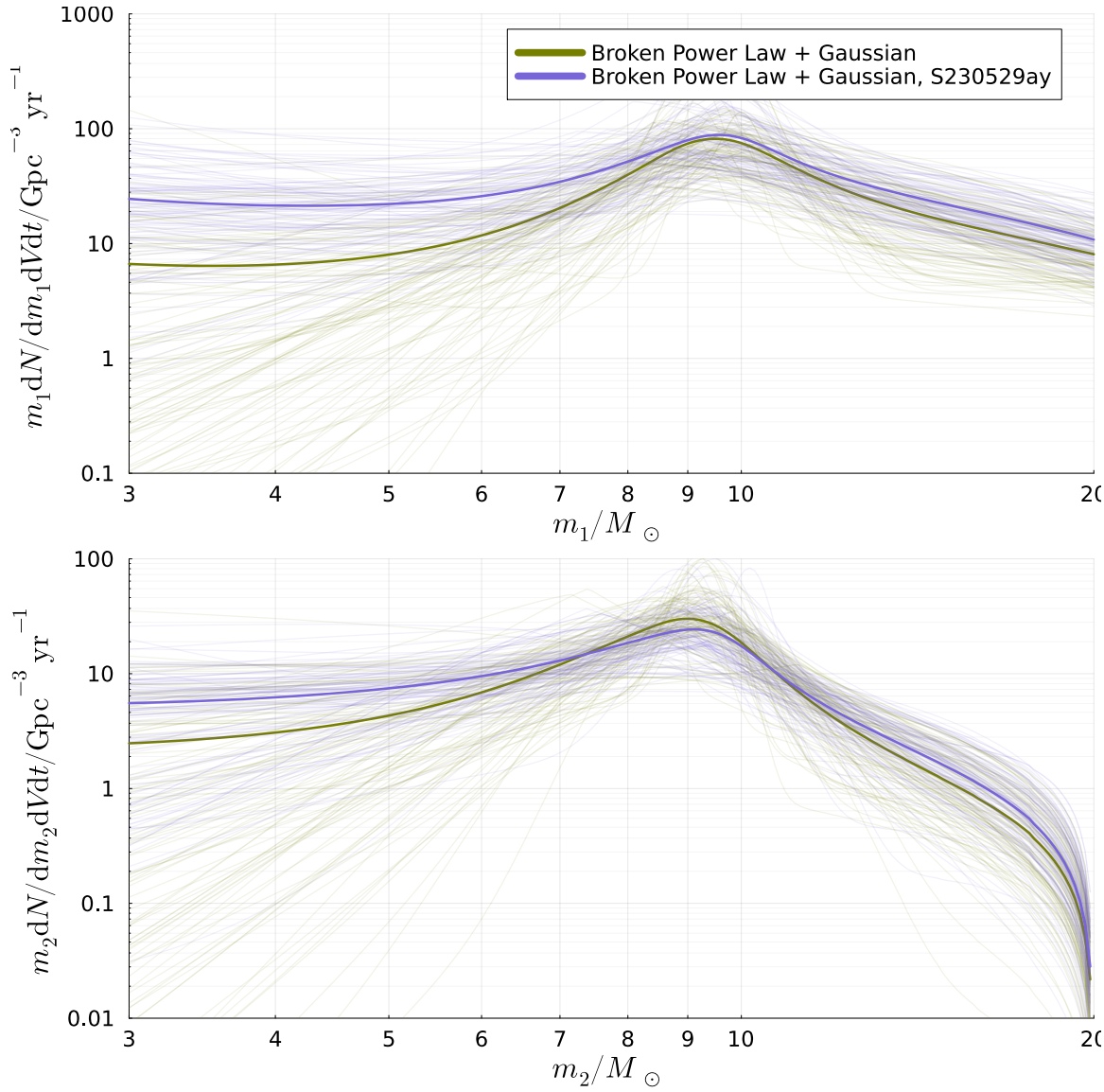

Figure 2. Inferred mass functions for $3\,M_\odot < m_2 < m_1 < 20\,M_\odot$ from two models; both primary and secodary (marginal) mass functions are shown. Dark lines show the posterior mean mass function; light lines are individual draws from the posterior over mass functions.

Table 1. $m_{1\%}$ for our various models and using different selection functions.

Mass Function Model	$m_{1\%}/M_\odot$ (1-σ, 68%)	$m_{1\%}/M_\odot$ range (2-σ, 95%)
`Broken PL`	$5.08^{+1.01}_{-1.24}$	$[3.2, 6.7]$
`Broken Power Law + Gaussian`	$3.61^{+1.63}_{-0.48}$	$[3.1, 6.4]$

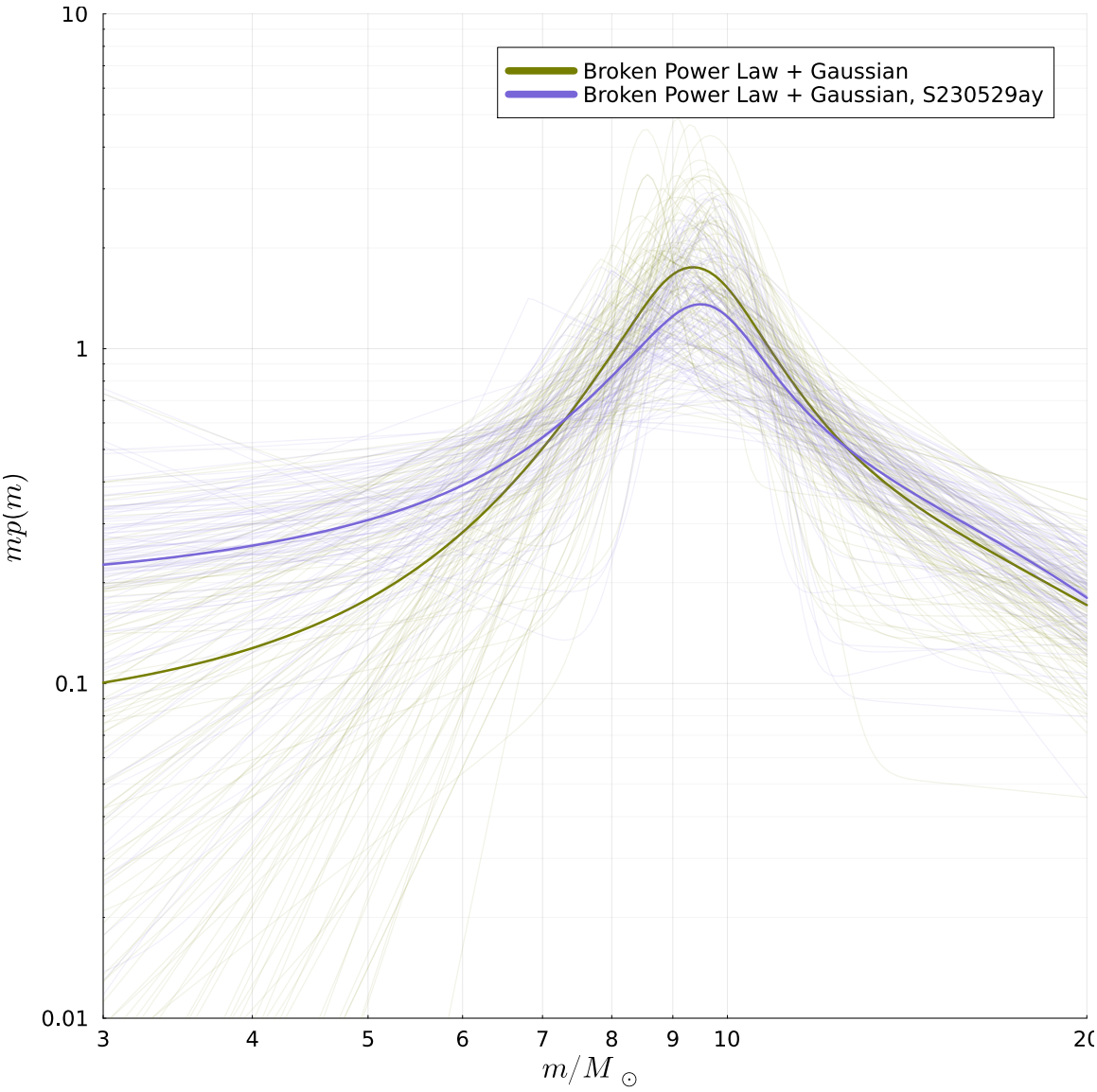

Figure 3. Inferred common mass distribution, $p(m)$, (see Eq. (7)) for both models considered in this analysis. Dark lines show the posterior mean mass distribution; light lines are individual draws from the posterior over mass distributions. At high masses, $m \gg \mu, m_b$, the mass function falls steeply in both models; the broken power law plus Gaussian slope $\alpha_2 = -2.2^{+1.3}_{-2.9}$. Toward lower masses from the peak, both power law models initially decline significantly, though the power law plus Gaussian model rises again as $m \to 3\,M_\odot$.

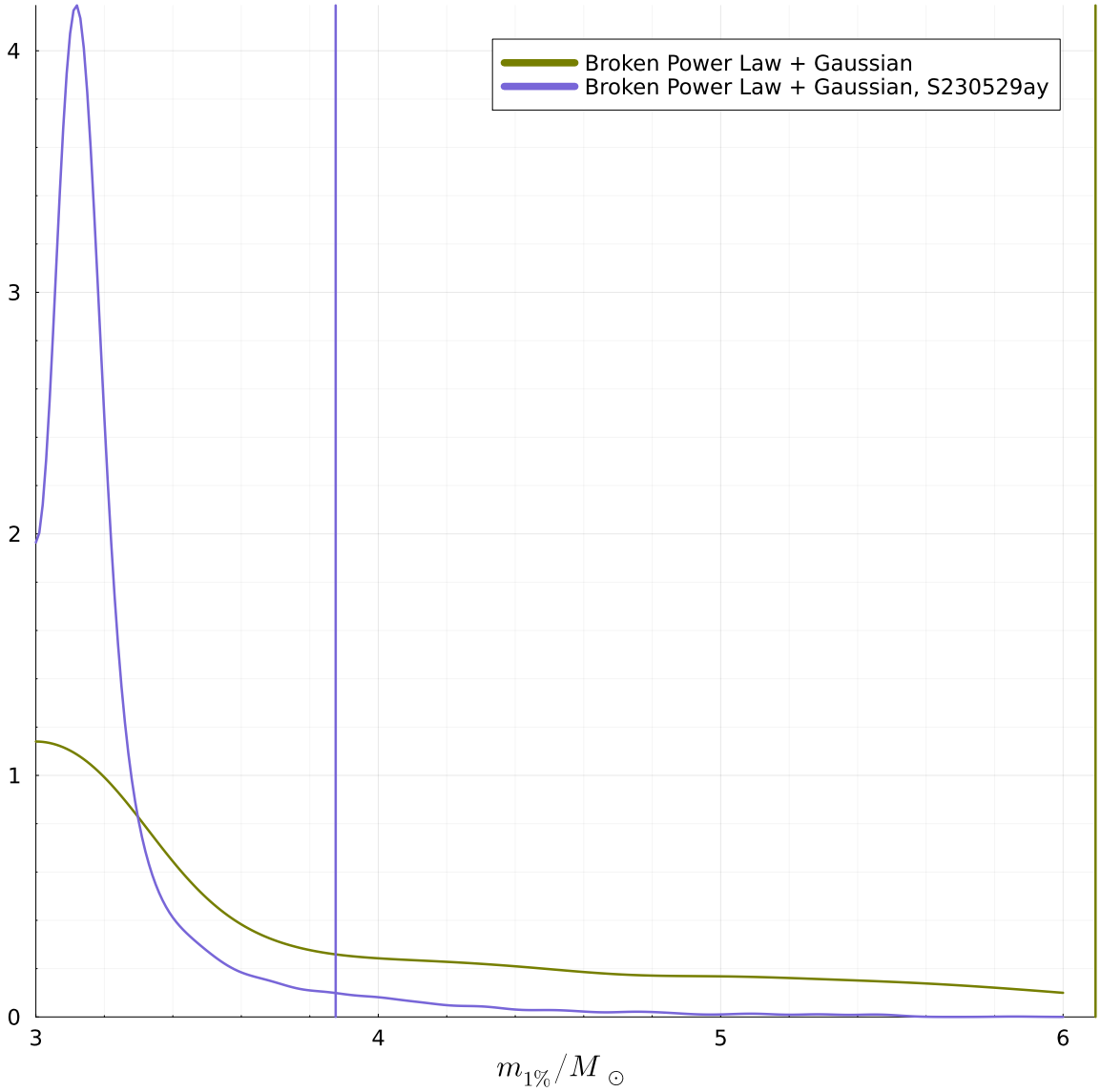

Figure 4. The posterior distribution for $m_{1\%}$, the first percentile of the "common" mass function for our three models. The broken power law plus Gaussian model with 50% selection cut has $m_{1\%} = 3.61^{+1.63}_{-0.48}\,M_\odot$ at 1σ (68%) credibility. The solid lines are the result for the 50% selection cut, dashed for the 90% selection cut.

REFERENCES

Fishbach, M., & Holz, D. E. 2020, ApJL, 891, L27, doi: 10.3847/2041-8213/ab7247

Madau, P., & Dickinson, M. 2014, ARA&A, 52, 415, doi: 10.1146/annurev-astro-081811-125615

Völgyes, D. 2020, Zenodo_get: a downloader for Zenodo records., doi: 10.5281/zenodo.1261812